



# A Series of Manganese(III) Salen Complexes as a Result of Team-Based Inquiry in a Transnational Education Programme

Danlei Yuan,<sup>[a, b]</sup> Ningqi Cai,<sup>[a, b]</sup> Jingxi Xu,<sup>[a, b]</sup> Danyang Miao,<sup>[a, b]</sup> Sheng Zhang,<sup>[a, b]</sup>  
Sian E. Woodfine,<sup>[a]</sup> Daniela Plana,<sup>\*,[a]</sup> Chris S. Hawes,<sup>\*,[a]</sup> and Michael Watkinson<sup>\*,[a]</sup>

The development of a team-based approach to research-led transnational practical chemistry teaching is described in which a team of five Chinese students on an articulated transnational degree programme, supported by a team of academic and technical staff, carried out a study examining the structural chemistry of a series of manganese(III) salen complexes. A series of four crystallographically characterized manganese(III) salen complexes with ancillary carboxylate ligands are reported here. The carboxylate coordination modes range from the bridging

*syn-anti*  $\mu^2$ - $\kappa\text{O}:\kappa\text{O}'$  mode observed in the predominant cyclohexanoate and isobutyrate species, to a capping terminal monodentate mode for the adamantanoate species, and an unusual mixture of bridging and terminal coordination modes observed in a second minor phase of the cyclohexanoate species. The variation on extended structures based on the weakly interacting aliphatic backbones may provide a useful basis for further structural studies.

## Introduction

Metallo-salen complexes and related species have found widespread utility in recent years, particularly in the field of asymmetric catalysis,<sup>[1]</sup> but also as biomimetic models, and in medical and materials applications.<sup>[2]</sup> Within this very broad class of systems manganese(III) salen complexes and their analogues have long been known as important catalytic species, epitomised by the seminal work of Jacobsen and Katsuki in the catalytic enantioselective epoxidation of a number of unfunctionalized alkenes.<sup>[3]</sup> In the 30 years since the first reports of the Jacobsen-Katsuki asymmetric epoxidation, a wide range of derivatives and analogues have been explored, with improved methods of asymmetric epoxidation and other

oxidation processes continuously under development.<sup>[4]</sup> Our interest in the field also began at this time when we were employing manganese(III) complexes of tetradentate  $\text{N}_2\text{O}_2$  donor Schiff base ligands as biomimetic models. During these studies we found that the nature of ancillary carboxylate ligands had a profound effect on the coordination chemistry observed.<sup>[5]</sup> Subsequently, we utilised the diverse array of carboxylate binding modes observed in these complexes to test the widely held validity<sup>[6]</sup> of assigning them through the use of vibrational spectroscopy.<sup>[7]</sup> The  $[\text{Mn}(\text{salen})]$  cation has also been widely used subsequently as a crystal engineering tecton, due to the nature of its linear building unit with two vacant coordination sites at the axial positions. These can be reliably occupied by bridging ligands, including carboxylates, as well as azides, cyanide and fluoride, to generate extended structures.<sup>[8]</sup> Control and modulation of the bridging modes in these systems is known to lead to interesting property relationships, influencing reactivity as well as the possibility of introducing electronic coupling between adjacent metal ions.<sup>[9]</sup> With the continued focus on the control of extended crystalline structures to access these properties,<sup>[10]</sup> particularly fuelled by the interest in coordination polymers and Metal-Organic Frameworks,<sup>[11]</sup> the  $[\text{Mn}(\text{salen})]$  cation is an attractive target for further study. Given our combined interests in manganese-Schiff base chemistry and crystal engineering<sup>[4a,12]</sup> we were attracted by the potential of their application in the practical provision of our transnational undergraduate programme.

Although not a new phenomenon, internationalisation has increasingly become important for the UK Higher Education (HE) sector, being one of the UK's most important export earners and contributing towards national wealth.<sup>[13]</sup> In the UK, transnational education (TNE) has continuously increased over a number of years, with an ever evolving landscape, including a wide variety of modalities adopted across the sector, from

[a] D. Yuan, N. Cai, J. Xu, D. Miao, S. Zhang, Dr. S. E. Woodfine, Dr. D. Plana, Dr. C. S. Hawes, Prof. M. Watkinson  
The Lennard Jones Laboratories  
School of Chemical and Physical Sciences  
Keele University  
Keele ST5 5BG (United Kingdom)  
E-mail: d.plana@keele.ac.uk  
c.s.hawes@keele.ac.uk  
m.watkinson@keele.ac.uk

[b] D. Yuan, N. Cai, J. Xu, D. Miao, S. Zhang  
Nanjing Xiaozhuang University  
Nanjing Shi  
Jiangsu Sheng (P. R. China)

Supporting information for this article is available on the WWW under <https://doi.org/10.1002/cplu.202000337>

This article is part of a Special Collection on "Supramolecular Chemistry: Young Talents and their Mentors". More articles can be found under [https://onlinelibrary.wiley.com/doi/toc/10.1002/\(ISSN\)2192-6506.Supramolecular-Chemistry](https://onlinelibrary.wiley.com/doi/toc/10.1002/(ISSN)2192-6506.Supramolecular-Chemistry).

© 2020 The Authors. Published by Wiley-VCH Verlag GmbH & Co. KGaA. This is an open access article under the terms of the Creative Commons Attribution License, which permits use, distribution and reproduction in any medium, provided the original work is properly cited.

branch campuses abroad to complete distance learning programmes, going through articulation agreements.<sup>[13,14]</sup> In particular, China has remained within the top 5 countries where UK TNE is delivered, with a marked increase in the number of UK-China joint HE initiatives in the last decade. This is due in part to Chinese economic reform, as well as by their willingness to adopt “Western” styles of teaching and learning within their own educational culture. The most common TNE model adopted between the two countries has been articulation programmes, where Chinese students spend 1 (or 2) year(s) of their full degree programme in a UK institution. In addition, during the years spent studying in China, UK-based faculty travel to deliver intensive teaching blocks, which are sometimes also supplemented with distance learning.<sup>[14–15]</sup> A particularly complex aspect of these programmes is the development of practical and transferable skills; in the Chinese courses, the focus tends to be on theory over practice, whereas in the UK, direct utilization by the students of the knowledge gained and links to real-world applications are heavily emphasised.<sup>[16]</sup>

In this study, we report the findings of a crystal engineering pilot study investigating the effect of backbone steric bulk on a series of manganese(III) tetradentate  $N_2O_2$  Schiff base carboxylate complexes, carried out with a group of students engaged in the Keele University – Nanjing Xiaozhuang University BSc Applied Chemistry programme. We explain how the design of the practical course content was augmented with research elements and how the experimental data were validated, and report the findings of the study itself which include the structures of four novel [Mn(salen)] complexes and detailed analysis of their solid-state structures.

## Results and Discussion

### Teaching Approach

The Keele-NXU BSc Applied Chemistry programme is an articulated 3+1 joint degree, full details of which have been previously published.<sup>[15,17,18]</sup> Briefly, the students are based in Nanjing Xiaozhuang University for the first three years, moving to the UK for their final year of study. Keele University staff deliver eight “bridging modules” during the second and third years of the programme, six in person, through “flying faculty”, and two as distance learning on-line modules. The last year consists of the NXU students essentially integrating into the final year of the BSc Chemistry programme at Keele, with the only exception being that the Chinese students do not undertake the Chemistry Research Project module. This is replaced by two specially designed lab-based modules, Applied Chemistry 1 and 2.

This approach was taken as Chinese students typically have limited previous experience in practical techniques, particularly in terms of instrumental analysis. Through minimal practical provision delivered as part of the bridging modules, and consultation with the UK-China Universities and Royal Society of Chemistry (RSC) transnational degrees network, the need for gradual development of the students’ practical skills was clearly identified. The laboratory-based content within the bridging modules is severely limited, in terms of time, but also availability of instrumental techniques and specialised software, familiarisation of the staff with the laboratory environment, and differences in regulations and requirements between the two countries.

In most UK HE programmes, student-led inquiry-based learning would be favoured over staff-led scripted experiments for practical laboratory-based modules during the final year;



Daniela Plana obtained her Chemistry degree from the Universidad Simón Bolívar, Venezuela, completed her PhD studies at the University of Manchester, UK, and took up a postdoctoral position at the University of Bristol. As a Lecturer at Keele University, she has become involved in chemical education research, particularly regarding international students, transnational education, team-based learning, feedback and the use of technology for teaching.



Chris Hawes completed his PhD at the University of Canterbury, New Zealand under the supervision of Prof. Paul Kruger in 2012. He subsequently went on to postdoctoral positions at Monash University, Australia and Trinity College Dublin, Ireland. He was appointed as a Lecturer at Keele University, UK in 2017, where his research involves ligand design for the development of new MOFs for carbon capture and chemical sensing applications, and using single crystal X-ray crystallography to explore the structural chemistry of coordination compounds.



Mike Watkinson was appointed as Head of School of Chemical and Physical Sciences at Keele University in 2018 after spending nearly twenty years at Queen Mary, University of London, where he started his independent academic career. He is also the current Chair of The Royal Society of Chemistry Interest Group in Macrocyclic and Supramolecular Chemistry. Throughout his career he has been committed to the mentoring and support of colleagues in both his own universities and the wider community and derives huge satisfaction from the successes they have achieved, despite the advice he has given them. This contribution to the Supramolecular Chemistry: Young Talents and their Mentors special collection came about from our ongoing efforts to support and enhance the experience of students in research-focused laboratory teaching. The work described here combines the research interests and experience of Daniela and Chris under Mike’s mentorship and project design.

with open-ended research at this level a specific requirement of professional accreditation bodies, such as the RSC.<sup>[19]</sup> However, as previously discussed,<sup>[20]</sup> there may be different levels within inquiry approaches and students should go through these different stages. Not only is prior knowledge key to teaching and learning, but prior learning experiences themselves shape the way students learn.<sup>[21]</sup> Consequently, in order to avoid 'problematizing' international students by simply expecting them to seamlessly adapt to the new learning environment and methods, the step between the teacher-led to the student-centred approach was facilitated by the instructional scaffolding embedded within the constructively aligned set of modules, taking the students from scripted experiments to an open-ended semester-long group research project, within the final year of their degree in the UK.

The first of the two lab-based modules was designed as a set of scripted laboratory practicals, spanning a wide range of areas of chemistry, acting not only as a stepping stone between two educational systems, but in reality as scaffolding of practical knowledge, where the students learned to use instrumental techniques and developed their experimental skills. The subsequent Applied Chemistry 2 module, during which the work presented here was developed, focused on open-ended, collaborative project work, providing clear scaffolding or alignment between a more structured, supportive learning environment in the first semester and more independent research work in the second.

As increased independent study was identified as a concern by Chinese students on TNE chemistry programmes,<sup>[18]</sup> collaborative projects were chosen as students would benefit from working in groups, rather than individually; team-based approaches have shown benefits, including the sharing of responsibilities, interaction and integration, learning from and supporting each other.<sup>[22]</sup> An added benefit of this approach is preparing them for future work environments or postgraduate studies, where research is typically a collaborative activity, making group work an essential graduate attribute in higher education.<sup>[23]</sup> Groups were supported throughout not only by academic supervisors on their specific project, but by the same module lead and technical member of staff throughout the full academic year, providing continuity and familiarity, leading to improved student support and gradual development of the required practical skills.

For this project, we designed a study of manganese(III) Schiff base complexes in which carboxylate co-ligands could be varied to probe the effect on the structure and properties of these compounds. This provided multiple avenues for exploration by the students, opportunities for a more diverse range of laboratory experiences, and the potential to generate multiple datasets simultaneously from a parallel approach within the group. Crystal engineering as a discipline works on the basis of wide-ranging studies involving parallel experimentation to discover and harness recurring synthons,<sup>[24]</sup> and useful data-points can be achieved from a well-designed screen of experimental conditions.<sup>[25]</sup> This lends itself well to the huge opportunities that exist in undergraduate research,<sup>[26]</sup> and our aim in this study was to establish a starting platform to build

upon and develop a larger experimental dataset of structural information in further student-led studies. Variables can include crystallization method, presence of co-formers, solvent/antisolvent mixtures, and compositional screens such as anion/cation composition, isosteric replacement or steric modification of a compound backbone. Here, a selection of Schiff base ligands (salen, salpn, and their 3,5-di-tert-butyl derivatives and carboxylate backbones with increasing levels of steric bulk (isopropyl, cyclohexyl, adamantyl) were used (Figure 1). From these, three new salen complexes were prepared and crystallised successfully, as well as the known manganese salpn isobutyrate complex which we had previously reported in 1999.<sup>[5d]</sup> As such, the salen complexes became the focus of the verification study.

Crystallisation can be a notoriously challenging technique to achieve reproducibly at all levels due to the huge number of experimental variables,<sup>[27]</sup> and this can be exacerbated in undergraduate research laboratories by both time constraints (in this case the complete research project module consisted of seven 5-hour laboratory sessions) and the relative inexperience of the researchers in crystallization methods. For these projects, we mitigated this by subsequently pursuing independent reproduction of the results originally obtained by the undergraduate students by an experienced researcher. In this way, the complete research team can streamline the discovery process using the results of the conditions screen carried out by the students to guide a subsequent, more detailed study, while independently verifying experimental conditions, and filling in the inevitable gaps in data collection from the time-constrained laboratory course. We followed a similar approach a year earlier,<sup>[28]</sup> when a group of 5 students from the 2017-18 NXU cohort were assigned three new ligands to prepare and crystallize as their zinc(II) complexes. In that study, the students optimized reaction conditions for both the ligand and complex synthesis, exploring their own hypotheses for both, while subsequent reproducibility work revealed a second isomeric form of one ligand and a further two crystalline phases of zinc complexes.

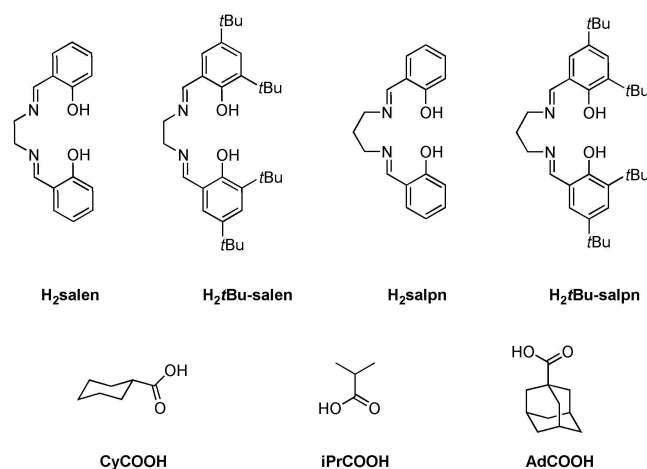


Figure 1. Structures of the ligands of interest to this study.

## Experimental Approach

### Preparation of the manganese precursors

The manganese carboxylate precursors were prepared following a similar method to that reported by Zhou *et al.*<sup>[29]</sup> We found that the isobutyrate and cyclohexanoate species could be prepared in good yield and with elemental analysis generally consistent with species of the type  $\text{Mn}(\text{RCOO})_2 \cdot x\text{H}_2\text{O}$ , although the formulations of similar compounds are known to vary and include oxides, protonated carboxylic acids and solvents.<sup>[30]</sup> In the absence of crystallographic evidence these formulations were taken as working assumptions. However, we found that adamantane-1-carboxylic acid suffered from poor solubility under these conditions and exhibited a tendency to foam, and the recovery of the subsequent manganese complex was in poor yield. Furthermore, elemental analysis of this species showed anomalously low carbon content and a C:H ratio inconsistent with a solvate of the bis-carboxylate compound, suggesting the presence of additional inorganics. The infrared spectrum of this species showed, beyond the main absorbances at 1491 and 1404  $\text{cm}^{-1}$ , several additional shoulders at 1540, 1614 and 1678  $\text{cm}^{-1}$ , as well as at least two overlapping absorbances in the range 1435–1454  $\text{cm}^{-1}$ , and is notably more complex than the carboxylate regions of the other salts (Figure S4 in the Supporting Information). Additional absorbances in both regions are consistent with carbonate or bicarbonate species.<sup>[31]</sup> Assuming an incomplete conversion of the carbonate starting material, the elemental analysis data are consistent with a mixed adamantanoate/carbonate formulation in a 2:1 ratio, or, alternatively, an adamantanoate/bicarbonate mixture of 1.25:0.75. Nonetheless, we were able to use all three precursors as convenient manganese-carboxylate sources to generate single crystals of the desired manganese(III) salen complexes.

### Synthesis and Structure of $[\text{Mn}(\text{salen})(\text{CyCOO})] \mathbf{1}$

Reaction of the manganese cyclohexanoate starting material with  $\text{H}_2\text{salen}$  in ethanol immediately gave a brown solution indicative of the expected oxidation to manganese(III). Several methods were attempted to crystallise this material, by diffusion of diethyl ether or toluene vapour, cooling the solutions, or slow evaporation. We found diethyl ether diffusion to be the most effective method, which yielded brown crystals over the space of one week at room temperature. In the initial screening performed by the students, we found an ethanol-solvated phase  $\mathbf{1-\alpha}$ ; however, subsequent reproduction and analysis of the bulk solid by X-ray powder diffraction indicated that this phase was only a minor constituent of the bulk (Figure S1 in the Supporting Information). When the reaction was repeated, the second (unsolvated) phase  $\mathbf{1-\beta}$  was also elucidated.

The diffraction data for  $\mathbf{1-\alpha}$  were solved and refined in the monoclinic space group  $P2_1/c$ , giving a structural model with an asymmetric unit containing two manganese ions coordinated

by two deprotonated salen ligands and two cyclohexanoate ligands, with one disordered lattice ethanol molecule present. As shown in Figure 2, each manganese ion is coordinated equatorially by a tetradentate salen ligand, though the nature of the axial interactions differs between the two sites. Manganese atom Mn1 adopts a regular octahedral coordination geometry with a monodentate carboxylate oxygen atom O5 occupying one site. The other position is occupied by oxygen atom O7 of a bridging *syn-anti* bis-monodentate ( $\mu^2-\kappa\text{O}:\kappa\text{O}'$ ) carboxylate which links through oxygen atom O8 to the second manganese site Mn2. While the two axial Mn–O bonds to Mn1 are both relatively long (2.218(2) and 2.216(2) Å for O5 and O7, respectively), Mn2 adopts a tighter 5-coordinate geometry, with an axial carboxylate Mn–O distance of 2.083(2) Å. A reciprocated close contact is also evident to the vacant axial coordination site from the phenolate oxygen atom O3 from an adjacent Mn-salen species, at a distance (Mn2–O3) of 2.550(2) Å.

As shown in Figure 3, when considering the dimerization of two dinuclear units, the overall structure of  $\mathbf{1-\alpha}$  can be considered as a discrete tetranuclear chain with bridging

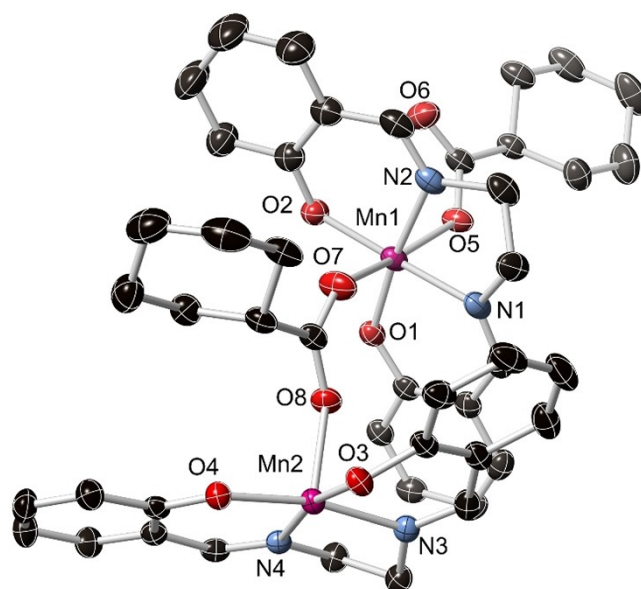


**Figure 2.** Structure of the dinuclear repeat unit of complex  $\mathbf{1-\alpha}$  with heteroatom labelling scheme. Hydrogen atoms and lattice ethanol molecules are omitted for clarity. ADPs are rendered at 50% probability.

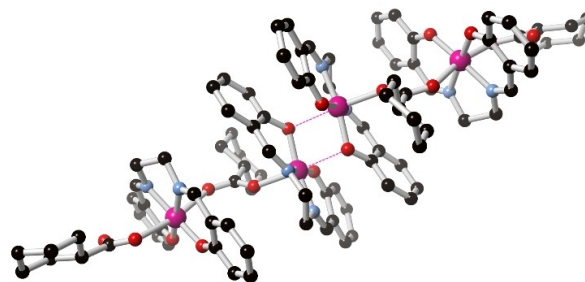


**Figure 3.** The complete tetranuclear unit of complex  $\mathbf{1-\alpha}$  showing the phenolate bridging between the two central  $[\text{Mn}(\text{salen})]$  units. Hydrogen atoms and ethanol solvent molecules are omitted for clarity.



through carboxylates and  $(\text{Mn-salen})_2$  dimers. The chains are capped by terminal monodentate carboxylates, which engage in hydrogen bonding with the lattice ethanol molecule through the non-coordinating oxygen atom O6. Interestingly, the two unique salen groups adopt slightly different geometries from one another. The salen group at the ends of the tetramer adopts a near-planar geometry; considering the mean planes of the two phenyl rings, the normal vectors of these planes are related by an angle of  $12.7^\circ$ , and a “fold” of  $8.1^\circ$ . However, the central salen unit adopts a much more folded geometry, with interplanar angle of  $24.9^\circ$  and fold of  $23.9^\circ$ . Here, the folding of the central salen is consistent with the steric clash between aromatic groups and the close approach between the phenolic oxygen atom and the adjacent manganese ion.

Each tetranuclear unit interacts with adjacent molecules through a series of weak non-covalent interactions. Visualisation through a normalized contact distance mapping on a Hirshfeld surface of the tetranuclear complex (Figure S5 in the Supporting Information)<sup>[32]</sup> shows the shortest internuclear distances involve the (disordered) ethanol solvent molecule, both in the form of the classical O–H...O hydrogen bond from the ethanol molecule, and also C–H...O contacts from several aromatic C–H groups to the ethanol oxygen atom. Additionally, the contoured surface of the tetramer allows for interdigitation between adjacent complexes; although no significant  $\pi$ – $\pi$  interactions are observed between complexes (discounting the close contact between the dimer at the centre of the complex), several instances of C–H...O interactions are observed, such as the contact between a salen methine C–H group and a coordinating carboxylate oxygen atom (C26...O5 distance 3.340(3) Å, C–H...O angle  $159^\circ$ ).

The structure of **1- $\beta$**  was determined after we discovered that the material prepared in our attempts to isolate a bulk sample of **1- $\alpha$**  was mostly comprised of a second phase. The X-ray diffraction data were solved and refined in the monoclinic space group  $P2_1/c$  (as with **1- $\alpha$** ). With a unit cell volume of less than half that of **1- $\alpha$**  ( $2025 \text{ \AA}^3$ , cf.  $4425 \text{ \AA}^3$  for **1- $\alpha$** ), we expected to find a single unique  $[\text{Mn}(\text{salen})]$  environment within the asymmetric unit. Indeed, the asymmetric unit of **1- $\beta$**  contains one salen ligand bound to a single manganese ion, with one cyclohexanoate ligand bound in the axial position and no lattice solvent molecules, as shown in Figure 4A. Expansion through crystallographic symmetry reveals a one-dimensional polymeric chain, with both axial manganese sites occupied by carboxylate oxygen atoms. The carboxylate ligand coordinates in a *syn-anti* bis-monodentate  $\mu^2$ - $\kappa\text{O}:\kappa\text{O}'$  coordination mode, similar to the bridging carboxylate in the structure of **1- $\alpha$** . The two axial Mn–O bonds are also comparable, at 2.193(2) and 2.214(2) Å for O3 and O4, respectively. However, each  $[\text{Mn}(\text{salen})]$  unit is subject to a twofold rotation about the *b* unit cell axis, which coincides with the polymeric chain direction. This contrasts with **1- $\alpha$** , where the carboxylate-bridged  $[\text{Mn}(\text{salen})]$  units are not symmetry-related and are twisted by  $114^\circ$  with respect to each other about the Mn1–Mn2 vector. The  $180^\circ$  twist in **1- $\beta$**  is more reminiscent of the bridging mode in the  $[\text{Mn}(\text{salpn})]$  acetate derivative,<sup>[5a]</sup> although in that instance

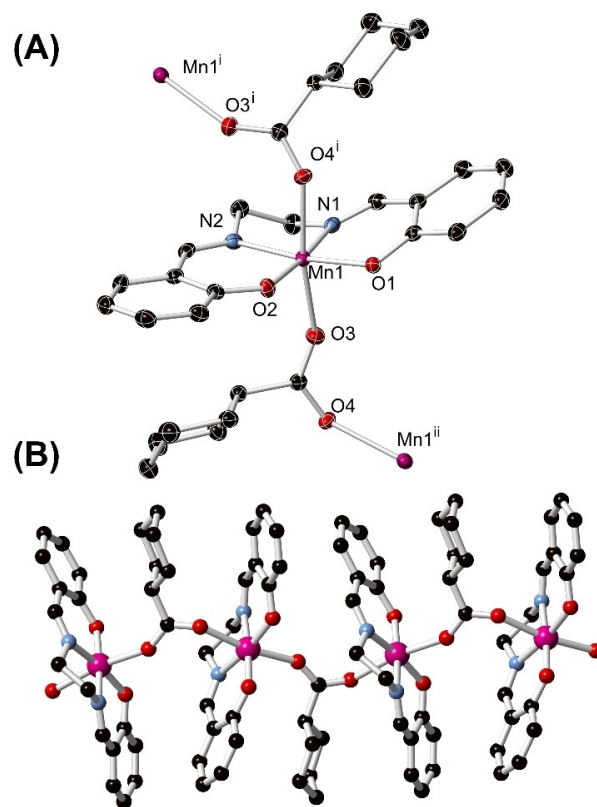


**Figure 4.** (A) The structure of complex **1- $\beta$**  and bridging mode to adjacent metal sites, with heteroatom labelling scheme. ADPs are rendered at 50% probability. (B) The packing of adjacent  $[\text{Mn}(\text{salen})]$  units via the *syn-anti* bridging mode of the cyclohexanoate ligand. All hydrogen atoms are omitted for clarity. Symmetry codes used to generate equivalent atoms: (i)  $1-x, \frac{1}{2}+y, \frac{1}{2}-z$ ; (ii)  $1-x, y-\frac{1}{2}, \frac{1}{2}-z$ .

desymmetrization is observed along the chain as a result of hydrogen bonding from lattice water molecules.

The more simplified extended structure of **1- $\beta$** , as shown in Figure 4B, provides some additional insights as to the crystal packing effects at play in these systems. Like the central unit in **1- $\alpha$** , the salen group adopts a folded conformation, with a fold angle of  $26.9^\circ$  and no twisting contribution. In this case, the folding of the salen group may relate to the close approach of adjacent salen groups along the polymeric chain, which includes angled C–H... $\pi$  contacts between aromatic groups, at a minimum C... $\pi$ (mean plane) distance of 3.33 Å for C12 to the C1–C6 plane at an interplanar angle of  $48.9^\circ$ . Several weak intramolecular C–H... $\pi$  contacts are also evident from the cyclohexyl group, which is flanked by two phenyl groups. Compared to **1- $\alpha$** , in **1- $\beta$**  the lack of both solvent of crystallisation and terminal carboxylate groups means considerably fewer opportunities for directed intermolecular interactions. While some C–H...O interactions are evident involving the phenolate oxygen atoms, the carboxylate oxygen atoms are largely shielded by the steric bulk of the salen groups. Likewise, with no externally-oriented  $\pi$  surfaces, there are no notable C–H... $\pi$  or  $\pi$ ... $\pi$  interactions between adjacent chains. This is in contrast to several similar carboxylate-bridged  $[\text{Mn}(\text{salen})]$  and  $[\text{Mn}(\text{salpn})]$  complexes and related species with smaller carbox-

ylate backbones,<sup>[5a,d,7]</sup> such as in our previously reported acetate and *n*-propanoate compounds, where interdigitation of adjacent chains was observed with C–H... $\pi$  or face to face  $\pi$ – $\pi$  interactions evident.

We made several attempts to generate the solvated 1- $\alpha$  phase in bulk, but were unsuccessful and continuously generated only trace quantities compared to the  $\beta$  phase. Interestingly, switching the reaction solvent from ethanol to methanol provided a third crystalline phase; single crystal X-ray diffraction showed this material to be [Mn(salen)(HCOO)], of the same polymorph reported by Ghosh.<sup>[33]</sup> The generation of formate under these reaction conditions, most likely from oxidation of methanol, is not without precedent in similar systems,<sup>[34]</sup> but may present an interesting opportunity for crystal engineering in the future.

### Synthesis and Structure of [Mn(salen)(iPrCOO)] 2

The reaction of salen with “[Mn*i*PrCOO]” under analogous conditions to those employed above gave a brown solution which deposited yellow-brown crystals following diffusion of diethyl ether vapour. Multiple repeats of the original synthesis reproducibly gave a single phase, and X-ray powder diffraction confirmed that the single crystal structure was indicative of the bulk. The diffraction data were solved in the orthorhombic space group  $P2_12_12_1$ , as an inversion twin. The structural model was refined to show the asymmetric unit contains one [Mn(salen)] unit and a single isobutyrate ligand, with no lattice solvent, as shown in Figure 5A.

The structure is closely comparable to 1- $\beta$  above; the isobutyrate ligand coordinates in a *syn-anti* bis-monodentate  $\mu^2$ - $\kappa O:\kappa O'$  mode, giving a one-dimensional coordination polymer oriented parallel to the *b* axis (Figure 5B). The two axial Mn–O bonds are statistically equivalent and similar to the equivalent bonds in 1- $\beta$  (2.206(2) and 2.195(2) Å for O4 and O3, respectively), while the phenyl-phenyl fold angle of 22.8° is also comparable to that described above. The twofold rotation relating adjacent [Mn(salen)] units along the propagation axis similarly blocks the majority of possible C–H...O interactions and other intra-chain contacts, and adjacent chains pack without significant directional forces between each. The sterics of the isobutyrate backbone are similar to the cyclohexyl, at least in the immediate vicinity of the carboxylic acid group, and so similar weak C–H... $\pi$  interactions are evident as the isopropyl group is sandwiched between two salen phenyl groups from the two bridged [Mn(salen)] units.

Given the close similarities between the unsolvated phase 1- $\beta$  and complex 2, we attempted a mixed-ligand experiment in which 0.5 equivalents of both manganese sources were combined with 1 equivalent of salen. This mixture was subjected to the same reaction and crystallisation conditions which had given rise to the original phases. Following diffusion of diethyl ether vapour, a small crop of yellow-brown crystals was obtained; analysis by X-ray powder diffraction (Figure S3 in the Supporting Information) showed that only 1- $\beta$  was formed

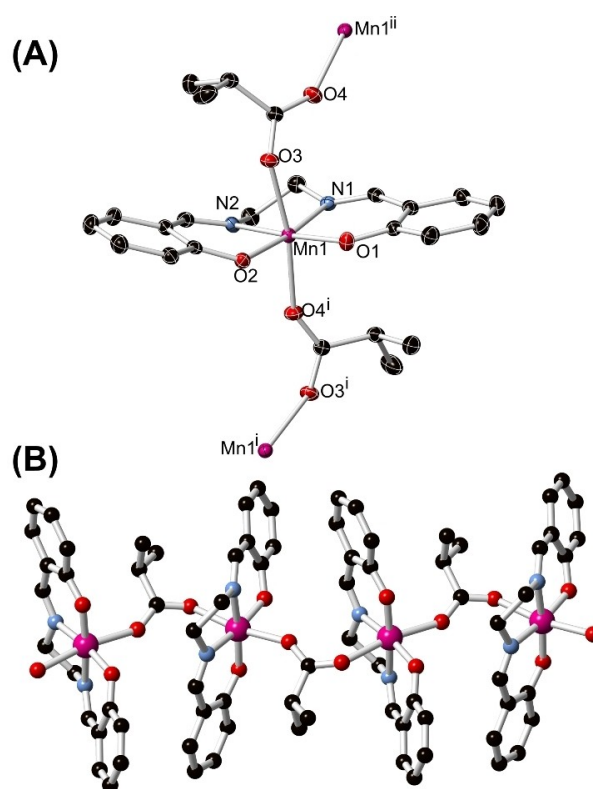


**Figure 5.** (A) The structure of complex 2 and bridging mode to adjacent metal sites, with heteroatom labelling scheme. ADPs rendered at 50% probability. (B) The packing of adjacent [Mn(salen)] units via the *syn-anti* bridging mode of the isobutyrate ligand, which is closely comparable to that observed in the cyclohexanoate case 1- $\beta$ . All hydrogen atoms are omitted for clarity. Symmetry codes used to generate equivalent atoms: (i)  $1-x, \frac{1}{2}+y, \frac{1}{2}-z$ ; (ii)  $1-x, y-\frac{1}{2}, \frac{1}{2}-z$ .

by this method, suggesting a mixed phase is not accessible under these conditions.

### Synthesis and Structure of [Mn(salen)(AdCOO)] 3

Reaction of the mixed adamantanoate/carbonate manganese source with salen gave a brown solution of similar appearance to the other complexes. Diffusion of diethyl ether vapour gave a mixture of two crystalline phases; one, yellow/brown rods of complex 3, was formed as a minor phase, while the dominant phase, a brown microcrystalline deposit intergrown with the minor phase, was formed unavoidably. Multiple reaction conditions were explored to avoid the formation of the second phase; the same outcome was observed with diffusion of diethyl ether, toluene, dichloromethane or ethyl acetate vapour, while slow evaporation or cooling of the alcohol solution failed to produce any crystalline material.

In all cases, we were unable to generate the pure adamantanoate complex 3 without the concurrent formation of the microcrystalline byproduct. Elemental analysis of the bulk (mixed) phase shows a low C:N ratio which is inconsistent with any substantial amount of adamantanoate being present in this material. The elemental analysis data are consistent with a

species of the general formula  $[\{\text{Mn}(\text{salen})(\text{EtOH})_2(\text{CO}_3)\}]$ , suggesting the presence of an inorganic anion in the major phase, though as we were unable to generate single crystals of this material its structure and connectivity is unclear. For the purposes of studying the solid-state structure of this material, a single crystal of **3** was manually separated from the mixture for X-ray diffraction.

The diffraction data for **3** were solved in the triclinic space group  $P\bar{1}$ , and the structure model contains a complete  $[\text{Mn}(\text{salen})(\text{AdCOO})]$  molecule in the asymmetric unit as shown in Figure 6. Unlike the structures of **1** and **2**, in complex **3** the manganese ion adopts a purely 5-coordinate geometry, with a shorter axial Mn–O bond to the monodentate carboxylate of 2.048(2) for Mn1–O3. The geometry of the manganese ion is best described as square pyramidal ( $\tau_5 = 0.1$ ),<sup>[35]</sup> although with the folded conformation (fold angle  $28.8^\circ$ ) adopted by the salen group both basal *trans* angles deviate from  $180^\circ$  ( $164.94(10)^\circ$  and  $159.01(10)^\circ$  for O2–Mn1–N1 and N2–Mn1–O1, respectively).

Despite the larger size of the adamantyl group, the lower coordination number in the structure of **3** allows for additional intermolecular contacts beyond those seen in the previous structures. Most notable are C–H...O interactions involving the carboxylate oxygen atoms, as shown in Figure 7. Adjacent complexes are linked by reciprocated C–H...O contacts from the methine carbon atom C10 to the non-coordinating carboxylate oxygen atom O4, at a C...O distance of 3.073(4) Å and C–H...O angle of  $158^\circ$ . The opposite end of the salen group participates in an unusual DDD...AAA motif of C–H...O contacts, where methylene, methine and phenyl C–H groups donate non-classical hydrogen bonds to the two carboxylate oxygen atoms and the phenolic oxygen atom, respectively. These interactions vary in their contact distances (3.616(4), 3.248(4) and 3.471(4) Å for C8...O4, C7...O3 and C5...O1, respectively) and C–H...O angles ( $159$ ,  $176$  and  $146^\circ$ , respectively), with the methine unsurprisingly acting as the most effective donor. Some limited face-to-

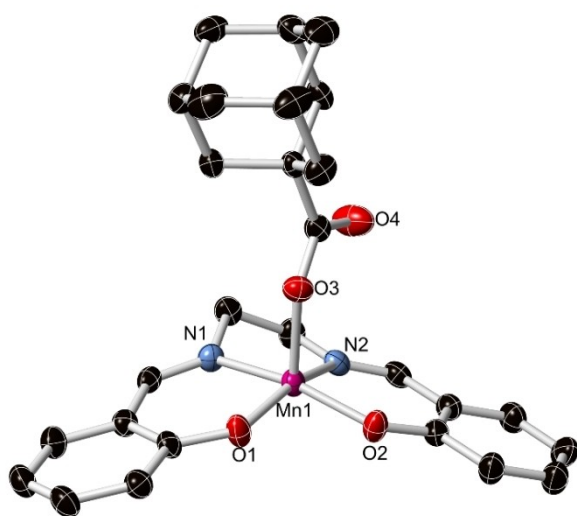


**Figure 6.** The structure of complex **3** with heteroatom labelling scheme. Hydrogen atoms are omitted for clarity. ADPs rendered at 50% probability.

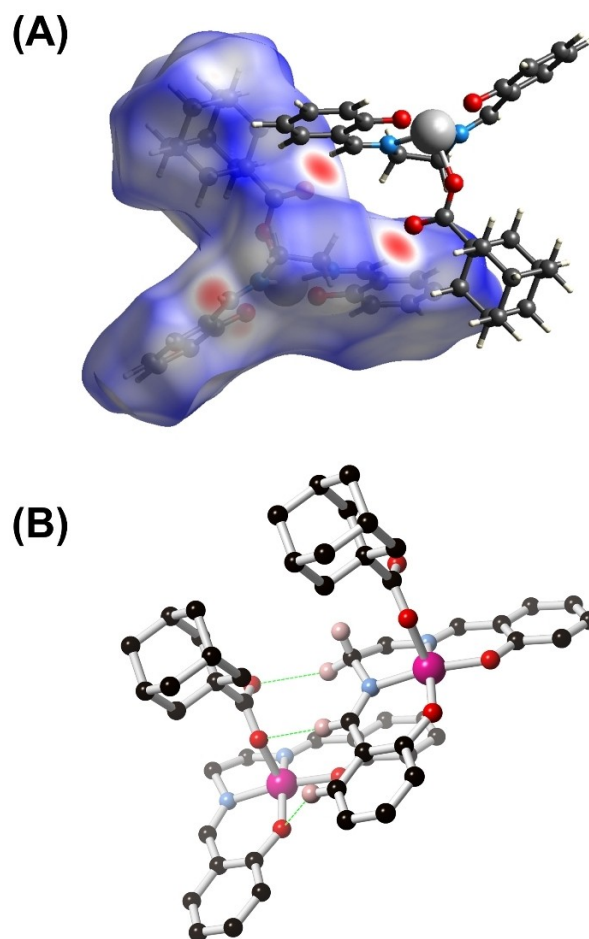


**Figure 7.** The main intermolecular interactions in the structure of complex **3**. (A) The reciprocated methine...carboxylate contacts between adjacent molecules represented on a normalized contact distance mapping of the Hirshfeld surface (rendered at surface isovalues  $-0.5/+1.3$ ). (B) The DDD...AAA set of weak C–H...O interactions between adjacent molecules in the structure of **3**, where the methine...carboxylate interaction is the most substantial.

face  $\pi\cdots\pi$  interactions are also evident in the structure of **3**, though these are limited to partial overlaps of the outer edges of the phenyl rings due to the bulk of the adamantyl group on one face and the concave bend of the salen species blocking close contacts to the other face.

## Conclusion

Through the scaffolded increase of inquiry-based laboratory work, the students were able to develop their practical skills through the first semester and worked well during their group research projects. The research presented here was particularly suited to this programme, and the team-based approach, as it provided the opportunity of parallel activities along multiple avenues of exploration, using a diverse range of laboratory techniques. The outcome of the course has been largely positive for the students, many of whom have progressed onto postgraduate degrees in the UK or at home in China.

From the structures of complexes **1- $\alpha$** , **1- $\beta$** , **2** and **3**, it is clear that large-scale structural changes in manganese salen complexes can be effected by modification of the carboxylate backbones. We observed similar *syn-anti*  $\mu^2$ - $\kappa\text{O}:\kappa\text{O}'$  coordination modes in both **1- $\beta$**  and **2**, leading to very similar one-dimensional coordination polymers, while the much larger adamantyl backbone seemingly restricted the bridging ability of the carboxylate, leaving a discrete 5-coordinate manganese species **3**. We also uncovered a minor solvated phase **1- $\alpha$**  which showed intermediate behavior of the axial carboxylate ligands, with both *syn-anti* bridging and terminal capping behavior observed. These results suggest a subtle energetic landscape exists in the crystallization of these species where axial ligands with intermediate steric bulk may give access to these bridging geometries selectively, opening the scope for a wider crystal engineering study, and potentially allowing new reactivity to be explored.

## Experimental Section

### Materials and Methods

All reagents, starting materials and solvents were purchased from Merck, Alfa Aesar or Fluorochem, were of reagent grade or higher, and were used as received. Salen was prepared according to published procedures.<sup>[36]</sup> Infrared spectra were measured using a Thermo Scientific Nicolet iS10 instrument with an ATR sampling accessory. Elemental analysis was performed with a Thermo Scientific Flash 2000 CHNS elemental analyser, with vanadium pentoxide as a combustion aid and calibrated against sulfanilamide. X-ray powder diffraction patterns were measured on a Bruker D8 Advance powder diffractometer equipped with a Cu-K $\alpha$  source ( $\lambda = 1.54178 \text{ \AA}$ ). Samples were mounted on a zero-background silicon crystal sample holder. All samples were measured at room temperature in the range  $2\theta = 5\text{--}55^\circ$ . Data were compared against the simulated patterns from the single crystal data, measured at 150 K.

### X-ray Crystallography

Crystal and refinement parameters are presented in Table S1. All data were collected using a Bruker D8 Quest ECO diffractometer equipped with a Mo K $\alpha$  source ( $\lambda = 0.71073 \text{ \AA}$ ). Crystals were mounted on Mitigen micromounts in NVH immersion oil, and all collections were carried out using  $\varphi$  and  $\omega$  scans, with data collection and reduction controlled with the Bruker APEX-3 suite of programs.<sup>[37]</sup> Multi-scan absorption corrections were applied using SADABS,<sup>[38]</sup> and the corrected intensity data were solved using the intrinsic phasing routine in SHELXT.<sup>[39]</sup> Structural models were refined on  $F^2$  with full-matrix least squares procedures in SHELXL operating within the OLEX-2 GUI.<sup>[40]</sup> All non-hydrogen atoms were refined with anisotropic displacement parameters, while hydrogen atoms were placed in riding positions and refined with isotropic displacement parameters equivalent to 1.2 or 1.5 times the isotropic equivalent of their carrier atom. Complex **2** was refined as a two-component inversion twin. Specific collection and refinement strategies are further outlined in the combined crystallographic information file. Deposition Number(s) 1994437 (**1- $\alpha$** ), 1994438 (**1- $\beta$** ), 199439 (**2**), 1994440 (**3**) contain the supplementary crystallographic data for this paper. These data are provided free of charge by the joint Cambridge Crystallographic Data Centre and Fachinfor-

mationszentrum Karlsruhe Access Structures service [www.ccdc.cam.ac.uk/structures](http://www.ccdc.cam.ac.uk/structures).

### Synthesis of the manganese carboxylate precursors

The manganese carboxylates were prepared following adapted literature procedures.<sup>[29]</sup> A suspension of manganese(II) carbonate in water (50 mg/mL) was heated at reflux in the presence of the corresponding carboxylic acid (3 equivalents) for 24 hours. After this period the solution was filtered hot, and the filtrate evaporated to dryness to give a white to pale pink solid. This solid was slurried in ice-cold acetonitrile, filtered and dried in air.

"[Mn-CyCOO]": Prepared following the general procedure from  $\text{MnCO}_3$  (3.0 g, 26 mmol) and cyclohexanecarboxylic acid (10 g, 78 mmol). Yield 1.87 g (22% based on Mn). Found C, 51.91; H, 7.04%; Calculated for  $[\text{Mn}(\text{CyCOO})_2] \cdot 0.75\text{H}_2\text{O}$  ( $\text{C}_{14}\text{H}_{22}\text{O}_4\text{Mn} \cdot 0.75\text{H}_2\text{O}$ ) C, 52.10; H, 7.34%;  $\nu_{\text{max}}(\text{ATR}, \text{cm}^{-1})$  3342 m br, 2924 s, 2851 m, 1682 w, 1538 s, 1413 s sh, 1359 m, 1343 m, 1325 m, 1280 m, 1225 m, 1181 w, 1137 w, 1074 w, 1037 w sh, 938 w, 923 w, 892 m, 875 w, 845 w, 801 w, 763 w.

"[Mn-iPrCOO]": Prepared following the general procedure from  $\text{MnCO}_3$  (3.0 g, 26 mmol) and isobutyric acid (7.2 mL, 78 mmol). Yield 5.4 g (84% based on Mn). Found C, 38.78; H, 5.80%; Calculated for  $[\text{Mn}(\text{iPrCOO})_2] \cdot \text{H}_2\text{O}$  ( $\text{C}_8\text{H}_{16}\text{O}_5\text{Mn}$ ) C, 38.88; H, 6.53%;  $\nu_{\text{max}}(\text{ATR}, \text{cm}^{-1})$  3395 m br, 2966 m, 2929 w, 2871 w, 1541 s, 1471 m, 1406 s sh, 1376 w, 1359 m, 1305 s, 1281 s, 1169 w, 1097 m sh, 926 m, 843 w, 760 w sh, 637 m.

"[Mn-AdCOO]": Prepared following a modified general procedure in which the total solvent volume was increased from 60 mL to 150 mL to allow for the very poor solubility of the starting material, from  $\text{MnCO}_3$  (2.0 g, 17 mmol) and 1-adamantanecarboxylic acid (9.3 g, 52 mmol). Analysis suggested that this material consists of a mixture of manganese adamantanoate and carbonate or bicarbonate. This material was used without purification for the subsequent reaction. Yield 450 mg (7%–9% based on Mn). Found C, 45.84; H, 6.52%; Calculated for  $[\text{Mn}(0.75\text{HCO}_3)(1.25\text{AdCOO})] \cdot 3\text{H}_2\text{O}$  ( $\text{C}_{14.5}\text{H}_{25.5}\text{O}_{7.75}\text{Mn}$ ) C, 45.98; H, 6.78%; Calculated for  $[\text{Mn}_2(\text{AdCOO})_2(\text{CO}_3)] \cdot 2\text{H}_2\text{O}$  ( $\text{C}_{23}\text{H}_{38}\text{O}_{11}\text{Mn}_2$ ) C, 46.01; H, 6.38%;  $\nu_{\text{max}}(\text{ATR}, \text{cm}^{-1})$  3355 m br, 2902 m sh, 2849 m, 1678 w, 1614 w, 1491 s sh, 1438 m sh, 1404 s, 1365 w, 1342 m, 1314 m, 1289 w, 1260 w, 1180 w sh, 1105 w, 1091 w, 977 w sh, 912 m, 810 m, 759 m br, 680 m.

### Synthesis of [Mn(salen)(CyCOO)] 1

$\text{H}_2\text{salen}$ <sup>[36]</sup> (50 mg, 190  $\mu\text{mol}$ ) and "[MnCyCOO]" (60 mg, 180  $\mu\text{mol}$ , 1 eq.) were combined in ethanol (10 mL), and the resulting brown solution was heated at reflux for 2 hours. On cooling to room temperature the solution was filtered, and the filtrate was subjected to diffusion of diethyl ether vapour for 1 week, giving dark yellow-brown crystals. Yield 21 mg (26%). X-ray powder diffraction (Figure S1 in the Supporting Information) confirmed that crystals isolated by this method give predominantly the  $\beta$ -phase with only trace amounts of the solvated  $\alpha$ -phase present. Found C, 61.24; H, 5.57; N, 6.47%; Calculated for  $[\text{Mn}(\text{salen})(\text{CyCOO})]$  ( $\text{C}_{23}\text{H}_{25}\text{N}_2\text{O}_4\text{Mn}$ ) C, 61.61; H, 5.62; N, 6.25%;  $\nu_{\text{max}}(\text{ATR}, \text{cm}^{-1})$  3020 m, 2964 s sh, 2910s, 2852 s, 1634 s, 1597 m, 1539 s, 1466 m, 1445 s sh, 1397 s sh, 1336 m, 1323 m, 1302 m, 1277 w, 1258 w, 1231 w, 1201 s sh, 1148 s, 1125 s, 1082 s, 1043 m, 1030 m, 972 m, 957 m, 900 s, 863 m, 855 m, 979 s, 751 s sh, 714 m, 646 m, 620 s.



### Synthesis of [Mn(salen)(iPrCOO)] 2

H<sub>2</sub>salen (50 mg, 190 μmol) and “[Mn-iPrCOO]” (40 mg, 162 μmol) were combined in ethanol (8 mL) and heated at reflux for 2 hours. On cooling to room temperature the brown solution was filtered, and the filtrate was subjected to diffusion of diethyl ether vapour for 1 week. After this period the resulting brown crystals were isolated by filtration. Yield 25 mg (38%). Found C, 58.33; H, 5.07; N, 7.37%; Calculated for [Mn(salen)(iPrCOO)] (C<sub>20</sub>H<sub>21</sub>N<sub>2</sub>O<sub>4</sub>Mn) C, 58.83; H, 5.18; N, 6.86%; ν<sub>max</sub>(ATR, cm<sup>-1</sup>) 2964w sh, 2903 m sh, 2851 m, 1631 s, 1597 m, 1539 s sh, 1466 m, 1442 m sh, 1409 m sh, 1383 m, 1364 m, 1335 m, 1300 m, 1276 w, 1230 w, 1199 m, 1145 s, 1126 m, 1082 m, 1043 m, 1029 m, 973 m sh, 957 m, 900 s, 863 m sh, 839 w, 796 s, 750 s sh, 682 m, 620 s. Phase purity was confirmed by X-ray powder diffraction (Figure S2 in the Supporting Information)

### Synthesis of [Mn(salen)(AdCOO)] 3

H<sub>2</sub>-Salen (50 mg, 190 μmol) and “[Mn-AdCOO]” (70 mg, 230 μmol) were combined in ethanol (10 mL) and heated at reflux for 2 hours. On cooling to room temperature, the brown solution was filtered and the filtrate subjected to diffusion of diethyl ether. After one week, a small quantity of brown rod crystals were formed as a minor phase, dispersed with a second, microcrystalline phase. An individual crystal for X-ray diffraction studies was isolated directly from this mixture. Elemental analysis of the bulk material is broadly consistent with the formulation {[Mn(salen)(EtOH)]<sub>2</sub>(CO<sub>3</sub>)}, with the adamantanoate product 3 present as a minor phase only. Found C, 55.43, H, 5.57, N, 7.57%; Calculated for {[Mn(salen)(EtOH)]<sub>2</sub>(CO<sub>3</sub>)} (C<sub>37</sub>H<sub>40</sub>N<sub>4</sub>O<sub>9</sub>Mn<sub>2</sub>) C, 55.93; H, 5.07; N, 7.05%.

### Acknowledgements

The authors gratefully acknowledge the School of Chemical and Physical Sciences, Keele University, for funding support. Parts of this work are supported by a Royal Society research grant to C.S.H. (Research Grant RGS\R1\191227). The authors also thank the UK-China Universities and RSC Transnational Degrees networks for useful discussions and support.

### Conflict of Interest

The authors declare no conflict of interest.

**Keywords:** crystal engineering · education · manganese · salen · team-based inquiry

- [1] S. Shaw, J. D. White, *Chem. Rev.* **2019**, *119*, 9381–9426.  
 [2] a) C. Freire, M. Nunes, C. Pereira, D. M. Fernandes, A. F. Peixoto, M. Rocha, *Coord. Chem. Rev.* **2019**, *394*, 103–134; b) S. Bosch, P. Comba, L. R. Gahan, G. Schenk, *Inorg. Chem.* **2014**, *53*, 9036–9051; c) R. Sanyal, X. Zhang, P. Kundu, T. Chattopadhyay, C. Zhao, F. A. Mautner, D. Das, *Inorg. Chem.* **2015**, *54*, 2315–2324; d) J. C. Pessoa, I. Correia, *Coord. Chem. Rev.* **2019**, *388*, 227–247; e) S. R. Doctrow, K. Huffman, C. B. Marcus, G. Tocco, E. Malfroy, C. A. Adinolfi, H. Kruk, K. Baker, N. Lazarowych, J. Mascarenhas, B. Malfroy, *J. Med. Chem.* **2002**, *45*, 4549–4558.  
 [3] a) W. Zhang, J. L. Loebach, S. R. Wilson, E. N. Jacobsen, *J. Am. Chem. Soc.* **1990**, *112*, 2801–2803; b) R. Irie, K. Noda, Y. Ito, N. Matsumoto, T. Katsuki, *Tetrahedron Lett.* **1990**, *31*, 7345–7348; c) E. M. McGarrigle, D. G. Gilheany, *Chem. Rev.* **2005**, *105*, 1563–1602; d) L. Kürti, M. M. Blewett, E. J. Corey, *Org. Lett.* **2009**, *11*, 4592–4595.  
 [4] a) A. Nodzewska, A. Wadolowska, M. Watkinson, *Coord. Chem. Rev.* **2019**, *382*, 181–216; b) M. Karmakar, S. Chattopadhyay, *J. Mol. Struct.* **2019**, *1186*, 155–186.  
 [5] a) N. Aurangzeb, C. E. Hulme, C. A. McAuliffe, R. G. Pritchard, M. Watkinson, A. Garcia-Deibe, M. R. Bermejo, A. Sousa, *J. Chem. Soc. Chem. Commun.* **1992**, 1524–1526; b) N. Aurangzeb, C. E. Hulme, C. A. McAuliffe, R. G. Pritchard, M. Watkinson, M. R. Bermejo, A. Sousa, *J. Chem. Soc. Chem. Commun.* **1994**, 2193–2195; c) C. E. Hulme, M. Watkinson, M. Haynes, R. G. Pritchard, C. A. McAuliffe, M. R. Bermejo, A. Sousa, *J. Chem. Soc. Dalton Trans.* **1997**, 1805–1814; d) M. Watkinson, M. Fondo, M. R. Bermejo, A. Sousa, C. A. McAuliffe, R. G. Pritchard, N. Jaiboon, N. Aurangzeb, M. Naeem, *J. Chem. Soc. Dalton Trans.* **1999**, 31–41; e) M. R. Bermejo, M. Fondo, A. Garcia-Deibe, A. M. Gonzalez, J. Sanmartin, A. Sousa, C. A. McAuliffe, R. G. Pritchard, M. Watkinson, I. Lukov, *Inorg. Chim. Acta*, **1999**, *293*, 210–217.  
 [6] G. B. Deacon, R. J. Phillips, *Coord. Chem. Rev.* **1980**, *33*, 227–250.  
 [7] D. Martínez, M. Motevalli, M. Watkinson, *Dalton Trans.* **2010**, *39*, 446–455.  
 [8] a) T. Birk, K. S. Pedersen, S. Pilgkios, C. A. Thuesen, H. Weihe, J. Bendix, *Inorg. Chem.* **2011**, *50*, 5312–5314; b) M. Yuan, F. Zhao, W. Zhang, Z.-M. Wang, S. Gao, *Inorg. Chem.* **2007**, *26*, 11235–11242; c) J. E. Davies, B. M. Gatehouse, K. S. Murray, *J. Chem. Soc. Dalton Trans.* **1973**, 2523–2527; d) H. Miyasaka, H. Takahashi, T. Madanbashi, K. Sugiura, R. Clérac, H. Nojiri, *Inorg. Chem.* **2005**, *44*, 5969–5971.  
 [9] N. Matsumoto, Y. Sunatsuki, H. Miyasaka, Y. Hashimoto, D. Luneau, J.-P. Tuchagues, *Angew. Chem. Int. Ed.* **1999**, *38*, 171–173; *Angew. Chem.* **1999**, *111*, 137–139.  
 [10] a) A. Mukherjee, *Cryst. Growth Des.* **2015**, *15*, 3076–3085; b) G. Resnati, E. Boldyreva, P. Bombicz, M. Kawano, *IUCr* **2015**, *2*, 675–690.  
 [11] G. Maurin, C. Serre, A. Cooper, G. Férey, *Chem. Soc. Rev.* **2017**, *46*, 3104–3107.  
 [12] a) V. D. Slyusarchuk, P. E. Kruger, C. S. Hawes, *ChemPlusChem* **2020**, *85*, 845–854; b) R. J. Weekes, C. S. Hawes, *CrystEngComm* **2019**, *21*, 5152–5163; c) A. Nodzewska, M. Watkinson, *Chem. Commun.* **2018**, *54*, 1461–1464.  
 [13] *The Scale and Scope of UK Higher Education Transnational Education*, HE Global, <http://www.universitiesuk.ac.uk/policy-and-analysis/reports/Documents/International/scale-and-scope-of-uk-he-tne.pdf> (Accessed 20/04/2020).  
 [14] K. Szkornik, *J. Geogr. Higher Educ.* **2017**, *41*, 521–531.  
 [15] J. Hyde, E. Page, P. Cranwell, *Educ. Chem.* **2016**, *53*, 22–25.  
 [16] a) F. Hyland, S. Trahar, J. Anderson, A. Dickens, *A Changing World: the internationalisation experiences of staff and students (home and international) in UK Higher Education*, The Higher Education Academy ESCalate, **2017**, Accessible from <http://escalate.ac.uk/4967>; b) J. Hyde in *Teaching Chemistry in Higher Education: A Festschrift in Honour of Professor Tina Overton* (Eds. M. K. Seery, C. McDonnell), Creathach Press, Dublin, **2019**, pp. 405–419.  
 [17] K. J. Haxton, R. J. Darton, *New Directions in the Teaching of Physical Sciences* **2019**, *14*, 2821.  
 [18] P. B. Cranwell, M. G. Edwards, K. J. Haxton, J. Hyde, E. M. Page, D. Plana, G. Sedhi, J. S. Wright, *New Directions in the Teaching of Physical Sciences* **2019**, *14*, 3325.  
 [19] *Accreditation of Degree Programmes*, The Royal Society of Chemistry, <http://www.rsc.org/Education/courses-and-careers/accredited-courses/> (Accessed 20/04/2020).  
 [20] M. K. Seery, A. B. Jones, W. Kew, T. Mein, *J. Chem. Educ.* **2019**, *96*, 53–59.  
 [21] P. Ramsden, *Learning To Teach in Higher Education*, Routledge, London, **1992**.  
 [22] a) K. J. Haxton, *The Journal of Academic Development and Education* **2016**, *5*, 41–50; b) A. Whiting, P. Gardner, F. Mair, M. Watkinson in *A Handbook for Teaching and Learning in Higher Education* (Eds. H. Fry, S. Ketteridge, S. Marshall), Kogan Page, London, **1999**, pp. 268–269.  
 [23] G. Sedghi, E. Rushworth, *New Directions in the Teaching of Physical Sciences* **2017**, *12*, 857.  
 [24] a) G. R. Desiraju, *J. Am. Chem. Soc.* **2013**, *135*, 9952–9967; b) G. R. Desiraju, *Angew. Chem. Int. Ed.* **2007**, *46*, 8342–8356; *Angew. Chem.* **2007**, *119*, 8492–8508.  
 [25] a) B. Spingler, S. Schnidrig, T. Todorova, F. Wild, *CrystEngComm* **2012**, *14*, 751–757; b) D. Braga, F. Grepioni, L. Maini, *Chem. Commun.* **2010**, *46*, 6232–6242; c) S. N. Black, E. A. Collier, R. J. Davey, R. J. Roberts, *J. Pharm. Sci.* **2007**, *96*, 1053–1068.  
 [26] R. LaDuca, J. J. Paul, G. Christou, *Polyhedron* **2006**, *114*, 1.

- [27] a) R.-Q. Chen, Q.-Q. Lu, Q.-D. Cheng, L.-B. Ao, C.-Y. Zhang, H. Hou, Y.-M. Liu, D.-W. Li, D.-C. Yin, *Sci. Rep.* **2015**, *5*, 7797; b) J. N. Sherwood, *Cryst. Growth Des.* **2004**, *4*, 863–877.
- [28] P. Chen, W. Ge, Y. Lu, Z. Wu, J. Xu, S. E. Woodfine, R. J. Darton, C. S. Hawes, *J. Coord. Chem.* **2019**, *72*, 1395–1416.
- [29] G.-J. Zhou, J. Richter, J. Schnack, Y.-Z. Zheng, *Chem. Eur. J.* **2016**, *22*, 14846–14850.
- [30] a) I. L. Malaestean, A. Ellern, P. Kögerler, *Eur. J. Inorg. Chem.* **2013**, 1635–1638; b) I. L. Malaestean, M. Speldrich, A. Ellern, S. G. Baca, M. Ward, P. Kögerler, *Eur. J. Inorg. Chem.* **2009**, 4209–4212.
- [31] M. Baldassarre, A. Barth, *Analyst* **2014**, *139*, 2167–2176.
- [32] a) M. A. Spackman, D. Jayatilaka, *CrystEngComm* **2009**, *11*, 19–31; b) J. J. McKinnon, D. Jayatilaka, M. A. Spackman, *Chem. Commun.* **2007**, 3814–3816.
- [33] P. Kar, R. Biswas, M. G. B. Drew, Y. Ida, Y. Ishida, A. Ghosh, *Dalton Trans.* **2011**, *40*, 3295–3304.
- [34] a) C. Cadiou, R. A. Coxall, A. Graham, A. Harrison, M. Helliwell, S. Parsons, R. E. P. Winpenny, *Chem. Commun.* **2002**, 1106–1107; b) X.-M. Zhang, *Coord. Chem. Rev.* **2005**, *249*, 1201–1219; c) K. E. Knope, H. Kimura, Y. Yasaka, M. Nakahara, M. B. Andrews, C. L. Cahill, *Inorg. Chem.* **2012**, *51*, 3883–3890.
- [35] A. W. Addison, T. Nageswara Rao, J. Reedijk, J. Van Rijn, G. C. Verschoor, *J. Chem. Soc. Dalton Trans.* **1984**, 1349–1356.
- [36] E. Solari, S. De Angelis, C. Floriani, A. Chiesi-Villa, C. Rizzoli, *J. Chem. Soc. Dalton Trans.* **1991**, 2471–2476.
- [37] Bruker APEX-3, Bruker-AXS Inc., Madison, WI, **2016**.
- [38] SADABS, Bruker-AXS, Madison, WI, **2016**.
- [39] G. M. Sheldrick, *Acta Crystallogr. Sect. A* **2015**, *71*, 3–8.
- [40] a) G. M. Sheldrick, *Acta Crystallogr. Sect. C* **2015**, *71*, 3–8; b) O. V. Dolomanov, L. J. Bourhis, R. J. Gildea, J. A. K. Howard, H. Puschmann, *J. Appl. Crystallogr.* **2009**, *42*, 339–341.

---

Manuscript received: April 27, 2020  
Revised manuscript received: May 12, 2020  
Accepted manuscript online: May 13, 2020